NORSAR

NORSAR Scientific Report No. 2-2005

Semiannual Technical Summary

1 January - 30 June 2005

Frode Ringdal (ed.)

Kjeller, August 2005

6.3 Surface Wave Tomography for the Barents Sea and Surrounding Regions

6.3.1 Introduction

Existing global and regional tomographic models have limited resolution in the European Arctic due to the small number of seismic stations, relatively low regional seismicity, and limited knowledge of the crustal structure. During the last decades, new seismic stations were permanently or temporarily installed in and around this region. However, many of the data from these stations are not easily accessible via the international data centers but only by direct request to the different data operators.

Recently, a new crustal model of the Barents Sea and the surrounding areas had been derived in a joint project of the University of Oslo, NORSAR and the USGS (Bungum *et al.*, 2004; 2005). This model, with its detailed information on crustal thickness and sedimentary basins in the area, is a valuable constraint for the tomographic inversion of the upper mantle velocity structure based on surface wave data.

6.3.2 Data collection

In this project, we have extensively searched for long period and broadband data observed at the seismic stations and arrays in the area from the beginning of the 1970s until 2005. We were able to retrieve surface wave observations from the data archives at NORSAR, University of Bergen, the Kola Science Center in Apatity, the Geological Service of Denmark and the University of Helsinki, in addition to the data, retrieved from the international data centers IRIS and GEOFON. The full list of used stations is given in Table 6.3.1 and a map with the positions of the stations is shown on top of Fig. 6.3.1.

In these data archives, not yet analyzed Love- and Rayleigh-wave data were identified and for more than 150 seismic events (earthquakes and nuclear explosions) dispersion curves were measured. The list of these events is presented in the Table 6.3.2 and the map on bottom of Fig. 6.3.1 shows the geographic distribution of the events.

6.3.3 Data analysis

From the surface wave recordings, group velocities of Love and Rayleigh waves were measured in the period range between10 and150 s using the program package for Frequency-Time Analysis developed at the University of Colorado (Ritzwoller & Levshin, 1998). After several cleaning procedures (Ritzwoller & Levshin, 1998), the new measurements were combined with the existing set of group velocity measurements provided by the Center for Imaging the Earth's Interior at the Colorado University (CU; see Levshin *et al.*, 2001). From this CU data set only those paths were selected, which were completely inside the cell [50 – 90° N, 60° W – 160° E], such that the entire data set consists of paths within the same regional frame. From cluster analysis (Ritzwoller & Levshin, 1998) of the root-mean-square of the group velocity measurements for the new data set in the considered period range was estimated as 0.010 – 0.015 km/s for Rayleigh waves and 0.015 – 0.025 km/s for Love waves.

To demonstrate the amount of new surface wave observations, we compare in Fig. 6.3.2 the number of newly analyzed Love and Rayleigh waves with the number in the preselected CU data set. Obviously, the new data set increased the ray density and consequently the resolution of the planned tomography. In particular for shorter periods, the number of rays crossing the target area was increased by more than 200% for Rayleigh waves and close to 200% for Love waves. For longer periods (*i.e.*, T > 80 s), the ratio of added data significantly drops since large seismic events, necessary to generate long period radiation, are very rare in this region.

6.3.4 2D-inversion for group velocity tomographic maps

A tomographic inversion for two-dimensional group-velocity maps has been done for a set of periods between 14 and 90 s following the procedure by Barmin *et al.*, 2001. In all cases, we inverted the combined data set of the newly acquired and analyzed data and the preselected CU data. As first results, we present in Figs. 6.3.3, 6.3.4, and 6.3.5 the resulting group-velocity maps for Love and Rayleigh waves at three different periods: 16, 25, and 40 s, respectively.

To illustrate the newly achieved, high path density, we also present in Figs. 6.3.3, 6.3.4, and 6.3.5 all ray paths of the newly acquired data for both, Love and Rayleigh waves on top of the figures. In the middle of the figures, we show these ray paths again but with all rays paths of the preselected CU data set on top. Note the many gaps in the preselected CU data set, for which group velocity information is now available.

The Love and Rayleigh group-velocity maps are shown at the bottom of Figs. 6.3.3, 6.3.4, and 6.3.5. The group-velocity maps derived from the combined data set, show the lateral deviation of the group velocities from the average velocity in percent. Note that these deviations are up to ±36% for Love and Rayleigh waves with a period of 16 s. This reflects the strong lateral heterogeneity of the Earth's crust in this region, which changes between the mid-oceanic ridge system (white line on the map), thick sedimentary basins in the Barents Sea, and old continental shields.

Sensitivity kernels for Love waves and Rayleigh waves are different; Rayleigh waves are sensitive for deeper structures than Love waves with the same signal period. Therefore, jointly analyzing the crustal structure with both Love and Rayleigh waves gives additional confirmation for an inverted velocity model. Note, *e.g.*, that the geographical pattern of group-velocity variations for Love waves at a period of 25 s (Fig. 6.3.4, on the right at the bottom) is similar to the pattern of group-velocity variations for Rayleigh waves at a period of 16 s (Fig. 6.3.3, on the left at the bottom). A similar relation is between the 40 s Love waves and the 25 s Rayleigh waves.

6.3.5 Further work: 3D-inversion for the shear velocity structure

The planned next step will be an inversion of all group-velocity maps (Love and Rayleigh waves) into a 3D shear-velocity model for the whole region (Shapiro & Ritzwoller, 2002). As additional constraints for thew inversion the thickness of the sedimentary layers and the Moho depth, as they were derived by Bungum *et al.* (2004; 2005) will be included. The result should yield a new, robust 3D model of the velocities in the upper mantle beneath the greater Barents Sea region down to about 250 km.

Acknowledgements

For this study we requested and retrieved broadband and long periodic data from the Norwegian National Seismic Network (NNSN, University in Bergen), Kola Regional Seismological Center (KRSC, Apatity), Danmarks og Grønlands Geologiske Undersøgelse (GEUS, Copenhagen), Totalförsvarets forskningsinstitut (FOI, Stockholm), British Geological Service (BGS, Edinburgh), the Finish National Seismic Network (FNSN, University of Helsinki), and the international network operators and data centers IRIS and GEOFON. That they all made their data available for this study is gratefully acknowledged.

Anatol Levshin, University of Colorado
Christian Weidle, University of Oslo
Johannes Schweitzer

References

Barmin, M. P., M. H. Ritzwoller & A. L. Levshin (2001). A fast and reliable method for surface wave tomography, *Pure Appl. Geophys.*, **158**, 1351-1375.

Bungum, H., O. Ritzmann, N. Maercklin, J. I. Faleide, W. D. Mooney & S. T. Detweiler (2005). Three-dimensional model for the crust and upper mantle in the Barents Sea region, *Eos. Trans. Am Geophys. Union*, **86**, 160-161.

Bungum, H., O. Ritzmann, J. I. Faleide, N. Maercklin, J. Schweitzer, W. D. Mooney, S. T. Detweiler & W. S. Leith (2004). Development of a three-dimensional velocity model for the crust and upper mantle in the Barents Sea, Novaya Zemlya and Kola-Karelia regions, in *Proceedings of the 26th Seismic Research Review: Trends in Nuclear Explosion Monitoring*, Orlando, FL (September 21 – 23, 2004).

Levshin, A. L., M. H. Ritzwoller, M. P. Barmin, A. Villaseñor & C. A. Padgett (2001). New constraints on the arctic crust and uppermost mantle: surface wave group velocities, P_n, and S_n, *Phys. Earth Planet. Int.*, **123**, 185-204.

Ritzwoller, M. H. & A. L. Levshin (1998). Eurasian surface wave tomography: Group velocities, *J. Geophys. Res.*, **103**, 4839-4878.

Shapiro, N. M. & M. H. Ritzwoller (2002). Monte-Carlo inversion for a global shear velocity model of the crust and upper mantle, *Geophys. J. Int.*, **151**, 88-105.

Table 6.3.1. List of seismic stations from which surface-wave data could be retrieved to increase the ray coverage in the Barents Sea and surrounding regions (see also Fig. 6.3.1). The abbreviations in the network-affiliation column stand for: AWI – Alfred-Wegener-Institute for Polar and Marine Research, BGS – British Geological Service, CNSN – Canadian National Seismograph Network, FNSN – Finish National Network (University in Helsinki), FOI – Totalförsvarets forskningsinstitut (Sweden), GEUS - Danmarks og Grønlands Geologiske Undersøgelse, GRSN – German Regional Seismic Network, IDA – International Deployment of Accelerometers, IMS – International Monitoring System, IRIS – Incorporated Research Institutions for Seismology, KRSC – Kola Regional Seismological Center, MASI99 – Temporal net of seismic stations in Finmark operated by NORSAR and the University of Potsdam (Germany), NNSN – Norwegian National Seismic Network (University in Bergen), RUB – Ruhr University Bochum, UK – University of Kiel, and USGS – US Geological Survey. The data availability for some of the stations may be longer than known to us.

Station	Latitude	Longitude	Location	Network Affiliation	LP or BB Data Availability
AMD	69.7420	61.6550	Amderma	KRSC	08.1998 -12.2003
APZ9	67.5686	33.4050	Apatity	KRSC	09.1992 -
ARE0	69.5349	25.5058	ARCES Array	NORSAR/IMS	09.1987 -
ARU	56.4302	58.5625	Arti	IRIS/IDA/IMS	09.1989 -
BER	60.3870	5.3348	Bergen	NNSN	01.2004 -
BILL	68.0651	166.4524	Bilibino	IRIS/USGS/IMS	08.1995 -
BJO1	74.5023	18.9988	Bjørn Øya (Bear Island)	NNSN	06.1996 -
BORG	64.7474	-21.3268	Borgarnes	IRIS/IDA	07.1994 -
BSD	55.1139	14.9147	Bornholm	GEUS	01.1996 -
COP	55.6853	12.4325	København	GEUS	09.1999 -
DAG	76.7713	-18.6550	Danmarkshavn	GEUS/GEOFON/AMI	06.1998 -
DSB	53.2452	-6.3762	Dublin	GEOFON	12.1993 -
EDI	55.9233	-3.1861	Edinburgh	BGS	06.1996 -
ESK	55.3167	-3.2050	Eskdalemuir	IRIS/IDA/BGS	09.1978 -
FIA1	61.4444	26.0793	FINES Array	FNSN/IMS	04.2001 -
HFC2	60.1335	13.6945	Hagfors Array	FOI/IMS	08.2001 -
HFSC2	60.1326	13.6958	Hagfors Array (closed)	FOI	01.1992 - 09.2003
HLG	54.1847	7.8839	Helgoland	UK/GEOFON	12.2001 -
IBBN	52.3072	7.7566	Ibbenbüren	RUB/GEOFON/GRSN	07.1999 -
JMI	70.9283	-8.7308	Jan Mayen (closed)	NNSN	10.1994 - 04.2004
JMIC	70.9866	-8.5057	Jan Mayen	NORSAR/IMS	10.2003 -
KBS	78.9256	11.9417	Ny-Ålesund	NNSN/AWI/GEOFON/ IRIS/USGS	10.1986 - 09.1987 11.1994 -
KEV	69.7553	27.0067	Kevo	FNSN/IRIS/USGS	10.1981 -
KIEV	50.6944	29.2083	Kiev	IRIS/USGS	01.1995 -
KONO	59.6491	9.5982	Kongsberg	NNSN/IRIS/USGS	09.1978 -
KWP	49.6305	22.7078	Kalwaria Paclawska	GEOFON	06.1999 -
LID	54.5481	13.3664	Liddow	GRSN/GEOFON	01.1994 - 11.1995
LRW	60.1360	-1.1779	Lerwick	BGS	08.2003 -
LVZ	67.8979	34.6514	Lovozero	IRIS/IDA	10.1992 -
MA00	69.5346	25.5056	at ARCES A0	MASI99	08.1999 - 10.1999
MA01	69.3752	24.2122	Suosjavrre	MASI99	05.1999 - 10.1999
MA02	69.1875	25.7033	Kleppe	MASI99	05.1999 - 10.1999
MA03	70.0210	27.3962	Sirma	MASI99	05.1999 - 10.1999
MA04	69.7127	29.5058	Neiden	MASI99	05.1999 - 10.1999
MA05	69.4533	30.0391	Svanvik	MASI99	05.1999 - 08.1999
MA06	70.4813	25.0609	Russenes	MASI99	05.1999 - 10.1999
MA07	69.7050	23.8203	Sautso	MASI99	05.1999 - 10.1999
MA08	70.1278	23.3736	Leirbotn	MASI99	05.1999 - 10.1999
MA09	69.4566	21.5333	Reisadalen	MASI99	05.1999 - 10.1999
MA10	69.5875	23.5273	Suolovuobme	MASI99	05.1999 - 10.1999

Station	Latitude	Longitude	Location	Network Affiliation	LP or BB Data Availability
MA11	68.6595	23.3219	Kivilompolo	MASI99	05.1999 - 10.1999
MA12	69.8349	25.0823	Skoganvarre	MASI99	05.1999 - 10.1999
MA13	70.3161	25.5155	Børselv	MASI99	05.1999 - 10.1999
MBC	76.2417	-119.3600	Mould Bay	CNSN/IMS	04.1994 -
MHV	54.9595	37.7664	Michnevo	GEOFON	05.1995 -
MOL	62.5699	7.5470	Molde	NNSN	11.2000 - 05.2001
MOR8	66.2852	14.7316	Mo i Rana	NNSN	05.2001 - 08.2002
MORC	49.7766	17.5428	Moravsky Beroun	GEOFON	11.1993 -
MUD	56.4559	9.1733	Mønsted	GEUS	12.1999 -
N1002	60.4438	10.3690	NORSAR Array	NORSAR	03.1971 - 09.1976
N1103	60.5911	10.1956	NORSAR Array	NORSAR	03.1971 - 09.1976
N1201	60.8008	10.0386	NORSAR Array	NORSAR	03.1971 - 09.1976
N1303	61.0281	9.9381	NORSAR Array	NORSAR	03.1971 - 09.1976
N1403	61.1527	10.3090	NORSAR Array	NORSAR	03.1971 - 09.1976
NAO01	60.8442	10.8865	NORSAR Array	NORSAR/IMS	03.1971 -
NB201	61.0495	11.2939	NORSAR Array	NORSAR/IMS	03.1971 -
NB302	60.9158	11.3309	NORSAR Array	NORSAR	03.1971 - 09.1976
NB400	60.6738	11.1881	NORSAR Array	NORSAR	03.1971 - 09.1976
NB504	60.5961	10.7794	NORSAR Array	NORSAR	03.1971 - 09.1976
NB603	60.6986	10.4358	NORSAR Array	NORSAR	03.1971 - 09.1976
NB701	60.9415	10.5296	NORSAR Array	NORSAR	03.1971 - 09.1976
NBO00	61.0307	10.7774	NORSAR Array	NORSAR/IMS	03.1971 -
NC204	61.2759	10.7629	NORSAR Array	NORSAR/IMS	03.1971 -
NC303	61.2251	11.3690	NORSAR Array	NORSAR/IMS	03.1971 -
NC405	61.1128	11.7153	NORSAR Array	NORSAR/IMS	03.1971 -
NC503	60.9075	11.7981	NORSAR Array	NORSAR	03.1971 - 09.1976
NC602	60.7353	11.5414	NORSAR Array	NORSAR/IMS	03.1971 -
NC701	60.4939	11.5137	NORSAR Array	NORSAR	03.1971 - 09.1976
NC800	60.4756	11.0868	NORSAR Array	NORSAR	03.1971 - 09.1976
NC902	60.4084	10.6872	NORSAR Array	NORSAR	03.1971 - 09.1976
NCO00	61.3374	10.5854	NORSAR Array	NORSAR	03.1971 - 09.1976
NOR	81.6000	-16.6833	Nord	GEUS/GEOFON	08.2002
NRE0	60.7352	11.5414	NORES Array	NORSAR	10.1984 - 06.2002
NRIL	69.5049	88.4414	Norilsk	IRIS/IDA/IMS	12.1992 -
NSS	64.5307	11.9673	Namsos	NNSN	10.2001 -
OBN	55.1138	36.5687	Obninsk	IRIS/IDA	09.1988 -
PUL	59.7670	30.3170	Pulkovo	GEOFON	05.‘995 -
RGN	54.5477	13.3214	Rügen	GRSN/GEOFON	12.1995 -
RUE	52.4759	13.7800	Rüdersdorf	GRSN/GEOFON	01.2000 -
RUND	60.4135	5.3672	Rundemannen	NNSN	03.1997 - 03.2003
SCO	70.4830	-21.9500	Ittoqqortoormiit (Scoresbysund)	GEUS	05.1999 -
SFJ	66.9967	-50.6156	Sondre Stromfjord	GEUS/IRIS/USGS/GEOFON	03.1996 -
SPB4	78.1789	16.3482	Spitsbergen Array	NORSAR/IMS	11.1992 -
STU	48.7719	9.1950	Stuttgart	GEOFON/GRSN	04.1994 -
SUMG	72.5763	-38.4540	Summit Camp	GEOFON	06.2002 -
SUW	54.0125	23.1808	Suwalki	GEOFON	11.1995 -
TIXI	71.6490	128.8665	Tiksi	IRIS/USGS/IMS	08.1995 -
TRO	69.6345	18.9077	Tromsø	NNSN	03.2003 -
TRTE	58.3786	26.7205	Tartu	GEOFON	06.1996 - 04.2003
VSU	58.4620	26.7347	Vasula	GEOFON	04.2003 -
WLF	49.6646	6.1526	Walferdange	GEOFON	03. 1994 -
YAK	62.0308	129.6812	Yakutsk	IRIS/USGS/IMS	09.1993 -

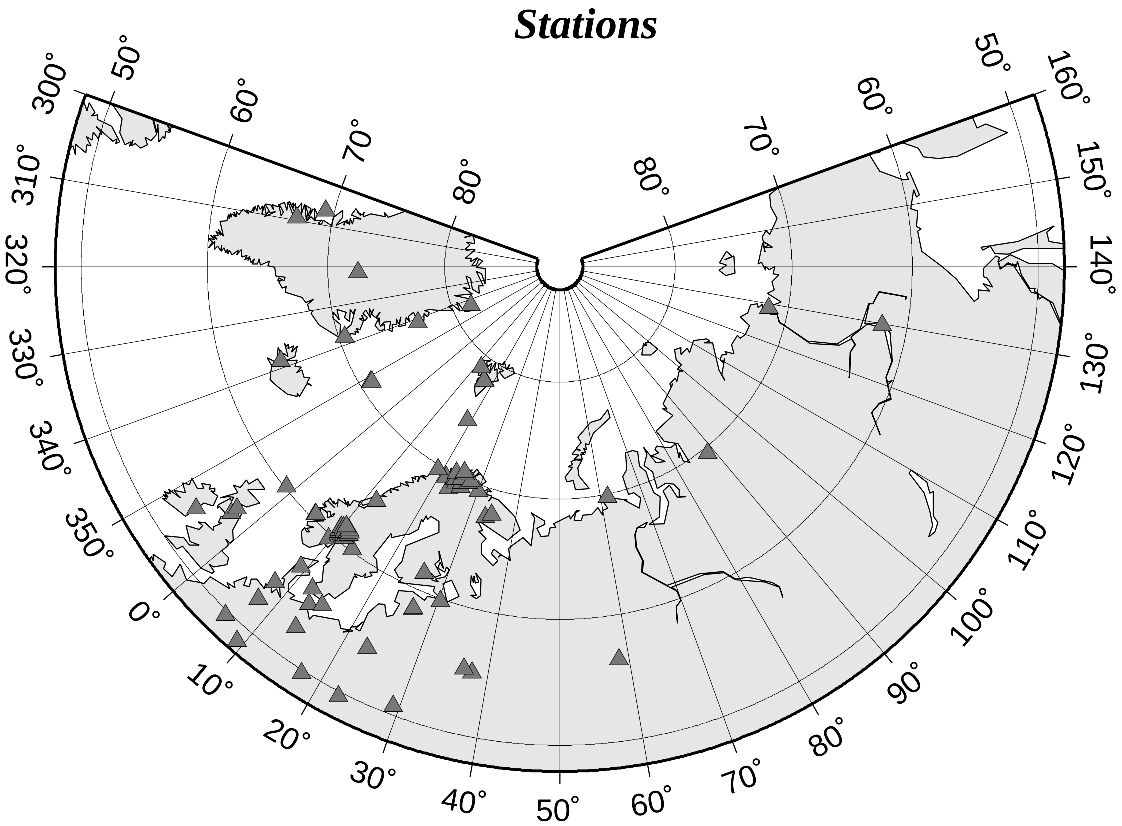

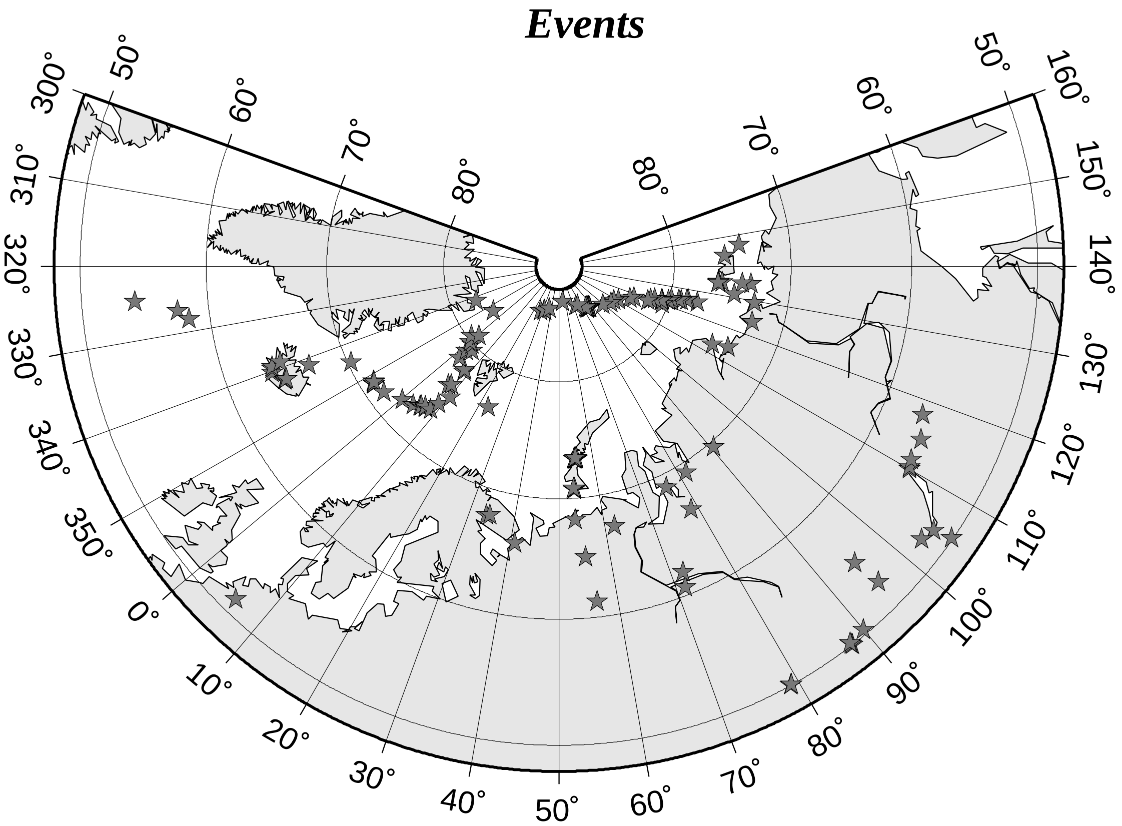

Fig. 6.3.1. The top map shows the seismic stations listed at Table 6.3.1 and the bottom map shows the distribution of the newly investigated seismic events as listed at Table 6.3.2.

Table 6.3.2. List with source parameters of the seismic events newly investigated during this study for measuring the group velocities of surface waves (Love and Rayleigh waves). A map with the event locations is shown in Fig. 6.3.1. All nuclear explosions investigated are marked with "expl".

Lat	Lon	Depth	Year	Month	Day	Time	mb	Ms	comment
61.2870	56.4660	0.0	1971	3	23	06:59:56.000	5.6	-	expl
73.3870	55.1000	0.0	1971	9	27	05:59:55.200	6.4	5.2	expl
73.3360	55.0850	0.0	1972	8	28	05:59:56.500	6.3	4.7	expl
52.3240	95.3660	33.0	1972	8	31	14:03:16.300	5.5	4.9	
73.3020	55.1610	0.0	1973	9	12	06:59:54.300	6.8	5.0	expl
70.7560	53.8720	0.0	1973	9	27	06:59:58.000	6.0	4.9	expl
64.7710	-21.0450	13.0	1974	6	12	17:55:08.700	5.5	5.3	
68.9130	75.8990	0.0	1974	8	14	14:59:58.300	5.5	-	expl
73.3660	55.0940	0.0	1974	8	29	09:59:55.500	6.4	5.0	expl
67.2330	62.1190	0.0	1974	8	29	14:59:59.600	5.2	-	expl
70.8170	54.0630	0.0	1974	11	2	04:59:56.700	6.7	5.3	expl
73.3690	54.6410	0.0	1975	8	23	08:59:57.900	6.4	4.9	expl
70.8430	53.6900	0.0	1975	10	18	08:59:56.300	6.7	5.1	expl
73.3510	55.0780	0.0	1975	10	21	11:59:57.300	6.5	-	expl
73.4040	54.8170	0.0	1976	9	29	02:59:57.400	5.8	4.5	expl
69.5320	90.5830	0.0	1977	7	26	16:59:57.600	4.9	-	expl
73.3760	54.5810	0.0	1977	9	1	02:59:57.500	5.7	-	expl
73.3360	54.7920	0.0	1978	8	10	07:59:57.700	5.9	4.3	
73.3800	54.6690	0.0	1978	9	27	02:04:58.200	5.6	4.5	expl
50.0460	78.9830	0.0	1978	11	4	05:05:57.500	5.6	4.2	expl
50.0530	79.0650	0.0	1979	7	7	03:46:57.400	5.8	-	expl
73.3690	54.7080	0.0	1979	9	24	03:29:58.300	5.7	-	expl
60.6770	71.5010	0.0	1979	10	4	15:59:57.900	5.4	-	
73.3380	54.8070	0.0	1979	10	18	07:09:58.300	5.8	-	expl
71.1920	-8.0300	10.0	1979	11	20	17:36:01.200	5.6	5.4	
73.3530	54.9970	0.0	1980	10	11	07:09:57.000	5.8	3.8	expl
68.2050	53.6560	0.0	1981	5	25	04:59:57.300	5.5	-	
73.3170	54.8120	0.0	1981	10	1	12:14:56.800	5.9	3.8	expl
69.2060	81.6470	0.0	1982	9	4	17:59:58.400	5.2	3.5	
73.3920	54.5590	0.0	1982	10	11	07:14:58.200	5.6	3.6	expl
73.3830	54.9130	0.0	1983	8	18	16:09:58.600	5.9	4.2	expl
73.3480	54.4950	0.0	1983	9	25	13:09:57.700	5.8	-	expl
65.0250	55.1870	0.0	1984	8	11	18:59:57.800	5.3	-	
61.8760	72.0920	0.0	1984	8	25	18:59:58.600	5.4	-	
67.7740	33.6880	0.0	1984	8	27	05:59:57.000	4.5	-	expl
73.3700	54.9550	0.0	1984	10	25	06:29:57.700	5.9	4.7	expl
65.9700	40.8630	0.0	1985	7	18	21:14:57.400	5.0	-	expl
63.8500	-19.7280	8.0	1987	5	25	11:31:54.300	5.8	5.8	
82.2290	-17.5560	10.0	1987	7	11	06:15:51.000	5.5	5.0	
73.3390	54.6260	0.0	1987	8	2	01:59:59.800	5.8	3.4	expl
74.6550	130.9620	10.0	1988	1	1	14:36:09.500	5.1	4.6	
77.6010	125.4510	10.0	1988	3	21	23:31:21.600	6.0	6.0	
73.3640	54.4450	0.0	1988	5	7	22:49:58.100	5.6	3.8	expl
66.3160	78.5480	0.0	1988	8	22	16:19:58.200	5.3	-	expl
73.3870	54.9980	0.0	1988	12	4	05:19:53.000	5.9	4.6	expl
71.1340	-7.6340	10.0	1988	12	13	04:01:38.900	5.7	5.6	
50.1030	105.3600	36.0	1989	5	13	03:35:02.800	5.6	5.6	
71.4320	-4.3710	10.0	1989	6	9	12:19:35.700	5.6	5.4	
76.1180	134.5780	10.0	1989	8	5	06:55:50.900	5.3	5.0	
76.1660	134.3460	13.0	1989	8	5	10:49:23.300	4.6	-	
76.1750	134.2460	10.0	1989	9	26	00:18:50.000	4.5	-	
80.6380	121.7610	31.0	1989	10	3	23:09:53.800	5.2	4.9	
80.5880	122.1320	10.0	1989	11	17	04:05:18.500	5.1	5.3	
73.3250	134.9090	18.0	1990	3	13	00:32:59.100	5.5	4.9	
74.2250	8.8280	29.0	1990	5	27	21:49:35.400	5.5	5.7	
75.0920	113.0960	33.0	1990	6	9	18:24:34.200	5.0	5.1	
64.6550	-17.6170	10.0	1990	9	15	23:07:42.800	5.5	5.2	
73.3610	54.7070	0.0	1990	10	24	14:57:58.100	5.7	4.0	expl
79.8490	123.8840	10.0	1991	3	22	17:02:19.500	4.7	4.1	
84.4010	108.2490	27.0	1991	6	11	07:16:34.400	5.5	5.3	

Lat	Lon	Depth	Year	Month	Day	Time	mb	Ms	comment
51.1530	5.7980	21.0	1992	4	13	01:20:00.800	5.5	5.2	
81.2460	121.2700	32.0	1992	6	8	09:30:16.100	5.1	4.6	
64.7800	-17.5940	10.0	1992	9	26	05:45:50.600	5.5	5.4	
86.9410	56.0730	10.0	1993	2	23	11:56:27.100	4.7	4.6	
64.5780	-17.4820	9.0	1994	5	5	05:14:49.700	5.7	5.2	
56.7610	117.9000	12.0	1994	8	21	15:55:59.200	5.8	5.8	
78.3020	2.3020	10.0	1995	3	9	07:04:22.100	5.1	4.4	
50.3720	89.9490	14.0	1995	6	22	01:01:19.000	5.5	5.2	
51.9610	103.0990	12.0	1995	6	29	23:02:28.200	5.6	5.5	
75.9840	6.9560	10.0	1995	10	4	09:17:30.200	5.1	4.9	
56.1000	114.4950	22.0	1995	11	13	08:43:14.500	5.9	5.6	
72.6440	3.4880	10.0	1995	12	8	07:41:12.700	5.2	5.2	
75.8200	134.6190	10.0	1996	6	22	16:47:12.910	5.6	5.5	
77.8600	7.5640	10.0	1996	8	20	00:11:00.340	5.3	5.0	
77.7460	7.8770	10.0	1997	2	6	14:41:51.750	5.3	-	
78.5100	125.5150	10.0	1997	4	16	08:42:27.550	4.8	4.3	
78.4450	125.8210	10.0	1997	4	19	15:26:33.480	5.7	5.0	
73.4170	7.9880	10.0	1997	10	6	21:13:10.380	5.0	-	
79.8880	1.8560	10.0	1998	3	21	16:33:11.000	5.9	6.1	
72.8260	129.5830	10.0	1998	8	23	09:59:02.970	4.5	-	
86.2830	75.6090	10.0	1998	10	18	22:09:19.160	5.2	4.6	
85.6410	86.1000	10.0	1999	2	1	04:52:40.810	5.1	4.7	
85.7340	84.4390	10.0	1999	2	1	09:56:35.020	5.1	5.2	
85.6050	85.8370	10.0	1999	2	1	11:55:15.070	4.5	-	
85.5710	87.1410	10.0	1999	2	1	11:56:00.800	5.1	5.5	
85.5730	87.0370	10.0	1999	2	19	19:10:00.540	5.1	5.0	
86.2780	73.3940	10.0	1999	2	22	08:02:11.170	5.2	4.8	
51.6040	104.8640	10.0	1999	2	25	18:58:29.400	5.9	5.5	
85.6860	86.0340	10.0	1999	3	1	17:46:46.340	5.0	5.0	
85.6920	84.7970	10.0	1999	3	13	01:26:33.540	5.3	5.1	
85.6340	86.8190	10.0	1999	3	21	15:24:07.840	5.4	5.1	
55.8960	110.2140	10.0	1999	3	21	16:16:02.200	5.5	5.7	
85.6820	85.7360	10.0	1999	3	28	21:32:29.650	4.4	-	
85.6440	86.2590	10.0	1999	3	28	21:33:44.090	5.0	5.1	
85.6480	86.5310	10.0	1999	4	1	10:47:53.010	5.1	5.1	
73.2150	6.6500	10.0	1999	4	13	02:09:22.270	5.0	4.7	
85.6720	84.8300	10.0	1999	4	26	13:20:07.620	5.2	4.9	
85.6320	86.1460	10.0	1999	5	18	20:20:16.060	5.1	5.3	
85.6050	86.5260	10.0	1999	5	26	23:56:32.670	5.1	4.6	
73.0170	5.1870	10.0	1999	6	7	16:10:33.630	5.3	5.4	
73.0770	5.4530	10.0	1999	6	7	16:35:46.700	5.2	5.3	
85.6040	83.7040	10.0	1999	6	11	23:54:52.000	5.1	4.5	
85.6770	85.7720	10.0	1999	6	18	19:47:25.180	5.3	4.8	
70.2800	-15.3510	10.0	1999	7	1	02:08:02.010	4.9	-	
85.7410	83.2640	10.0	1999	7	8	19:25:10.520	5.0	4.6	
72.2610	0.3960	10.0	1999	8	3	13:55:41.410	5.0	5.1	
67.8630	34.3790	10.0	1999	8	17	04:44:35.950	4.6	-	
79.2210	124.3970	10.0	1999	10	27	05:05:07.180	4.8	4.5	
55.8300	110.0290	10.0	1999	12	21	11:00:48.870	5.5	5.0	
80.6150	122.1300	10.0	1999	12	26	08:39:48.390	4.7	-	
80.5820	122.2510	10.0	1999	12	30	06:46:55.250	4.7	4.4	
79.8020	123.0760	10.0	2000	1	16	12:29:12.630	4.5	3.8	
75.2710	10.1950	10.0	2000	2	3	15:53:12.960	5.5	5.0	
79.8900	0.4380	10.0	2000	2	12	09:05:06.630	5.0	4.7	
71.1900	-8.2630	10.0	2000	5	21	19:58:47.410	5.3	5.6	
63.9660	-20.4870	10.0	2000	6	17	15:40:41.730	5.7	6.6	
63.9800	-20.7580	10.0	2000	6	21	00:51:46.880	6.1	6.6	
74.3330	146.9720	10.0	2000	7	10	04:17:36.830	4.6	3.9	
78.9680	124.4680	10.0	2000	9	16	17:45:17.820	4.6	-	
54.7070	94.9830	33.0	2000	10	27	08:08:53.540	5.6	5.3	
81.5320	120.2790	27.3	2000	12	31	01:45:03.240	5.1	4.5	
80.0380	122.7240	10.0	2001	4	8	02:59:03.880	4.5	-	
80.4640	120.0940	10.0	2001	5	1	23:44:57.170	4.5	-	
82.9330	117.5090	10.0	2001	5	30	15:19:04.350	4.7	-	
72.6750	124.0160	61.5	2001	6	8	04:59:05.250	4.7	-	

Lat	Lon	Depth	Year	Month	Day	Time	mb	Ms	comment
79.5140	4.1880	10.0	2001	7	16	14:09:29.240	5.0	4.5	
80.8480	0.7680	10.0	2001	12	8	06:44:22.020	5.1	4.8	
85.8580	27.6810	10.0	2002	5	3	11:19:20.320	4.1	-	
86.0050	31.5950	10.0	2002	5	3	11:20:51.540	5.2	5.4	
85.9720	31.1490	10.0	2002	5	3	15:33:34.880	5.1	5.1	
86.2760	37.1770	10.0	2002	5	28	15:39:01.550	4.9	4.7	
75.6340	143.7460	10.0	2002	6	4	00:05:07.170	4.8	-	
84.0830	110.6900	10.0	2002	6	9	21:20:38.750	4.5	-	
83.1360	-6.0780	10.0	2002	9	11	04:50:32.860	5.2	5.2	
66.9380	-18.4560	10.0	2002	9	16	18:48:26.720	5.5	5.7	
58.3110	-31.9460	10.0	2002	10	7	20:03:54.580	4.9	5.5	
57.4490	-33.3440	10.0	2003	2	1	18:47:52.150	5.3	5.5	
71.1220	-7.5770	10.0	2003	6	19	12:59:24.410	5.6	5.0	
76.3720	23.2820	10.0	2003	7	4	07:16:44.720	5.7	5.1	
73.2730	6.4210	10.0	2003	8	30	01:04:42.340	5.0	4.8	
56.0620	111.2550	10.0	2003	9	16	11:24:52.220	5.2	5.7	
80.3140	-1.8280	10.0	2003	9	22	20:45:16.910	5.2	4.7	
50.0380	87.8130	16.0	2003	9	27	11:33:25.080	6.5	7.5	
50.0910	87.7650	10.0	2003	9	27	18:52:46.980	6.1	6.6	
50.2110	87.7210	10.0	2003	10	1	01:03:25.240	6.3	7.1	
79.1410	2.3290	10.0	2003	10	7	02:36:54.440	5.1	4.6	
74.0800	134.8210	10.0	2003	12	7	09:16:12.640	5.0	4.4	
84.4750	105.2150	10.0	2004	1	19	07:22:52.910	5.5	5.2	
71.0670	-7.7470	12.2	2004	4	14	23:07:39.940	5.8	5.6	
81.7290	119.2920	10.0	2004	6	24	22:12:37.160	4.7	-	
54.1310	-35.2590	10.0	2004	7	1	09:20:44.140	5.4	5.5	
73.8300	114.4820	10.0	2004	10	2	11:06:01.470	4.5	-	
83.2630	115.9400	10.0	2004	11	13	21:28:01.450	4.6	-	
76.1690	7.5280	10.0	2004	11	27	06:38:29.290	5.0	4.5	
84.9480	99.3100	10.0	2005	3	6	05:21:43.430	6.1	6.2	

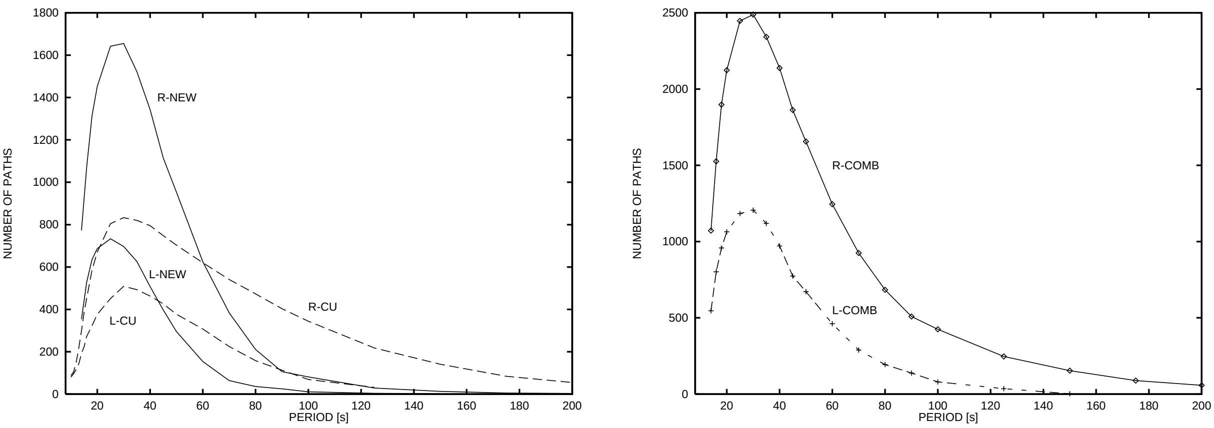

Fig. 6.3.2. The figure on the left shows the number of observed ray paths, on which Love- (L) and Rayleigh-wave (R) group velocities were measured for the preselected Colorado University data set (dashed lines, R-CU and L-CU) and during this new study (R-NEW and L-NEW). The figure on the right shows the number of ray paths in the joint data set used for the inversions in this study.

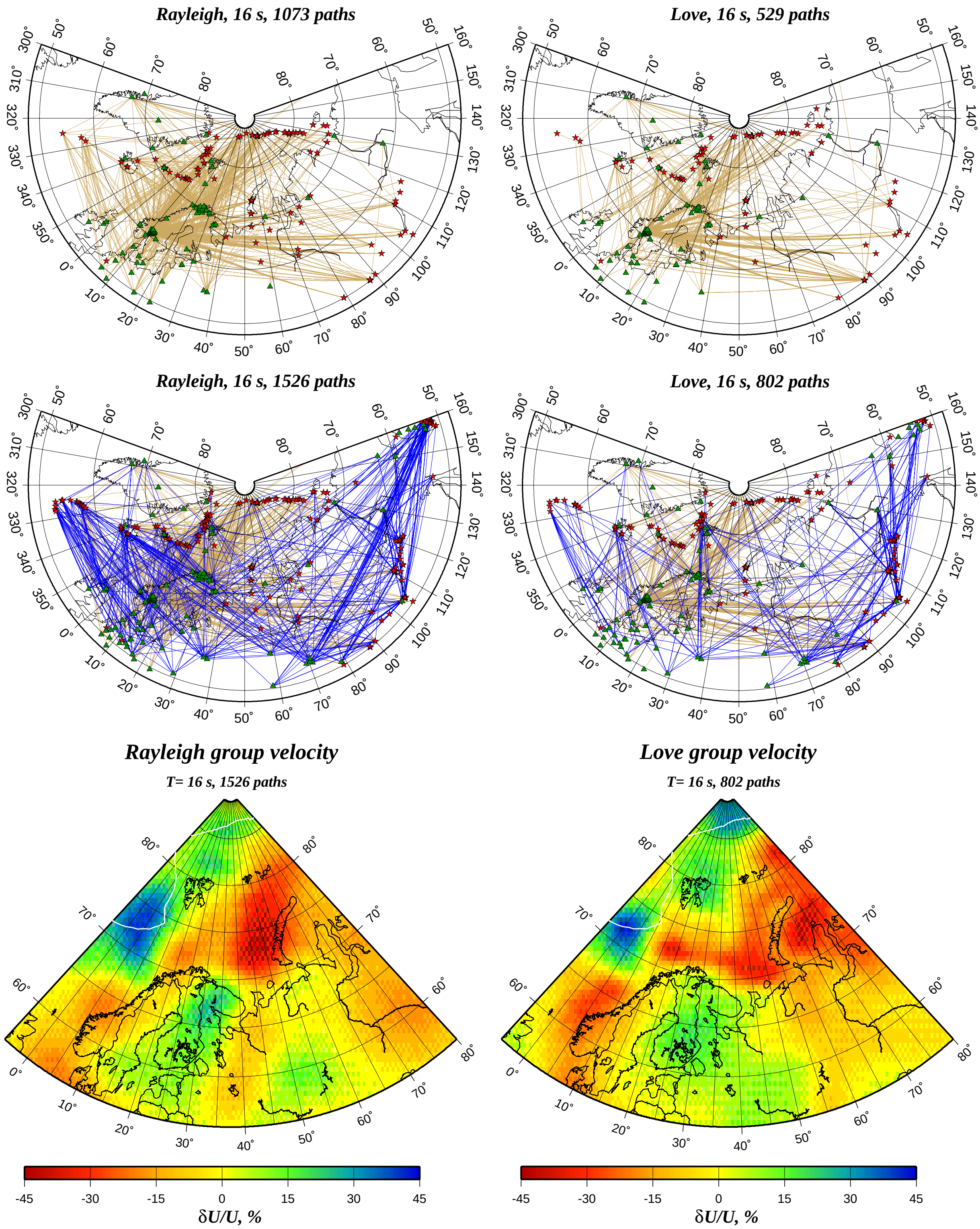

Fig. 6.3.3. Results of the 2D inversion for the group velocities of Love (on the right) and Rayleigh waves (on the left) with a period of 16 s. The two maps at the top show the ray coverage of the newly analyzed data. The two maps in the middle show the same rays plus the rays for the data from the preselected CU data set (blue). The two maps at the bottom present the 2D distribution of the inverted group velocities as deviations from the average velocity (in percent).

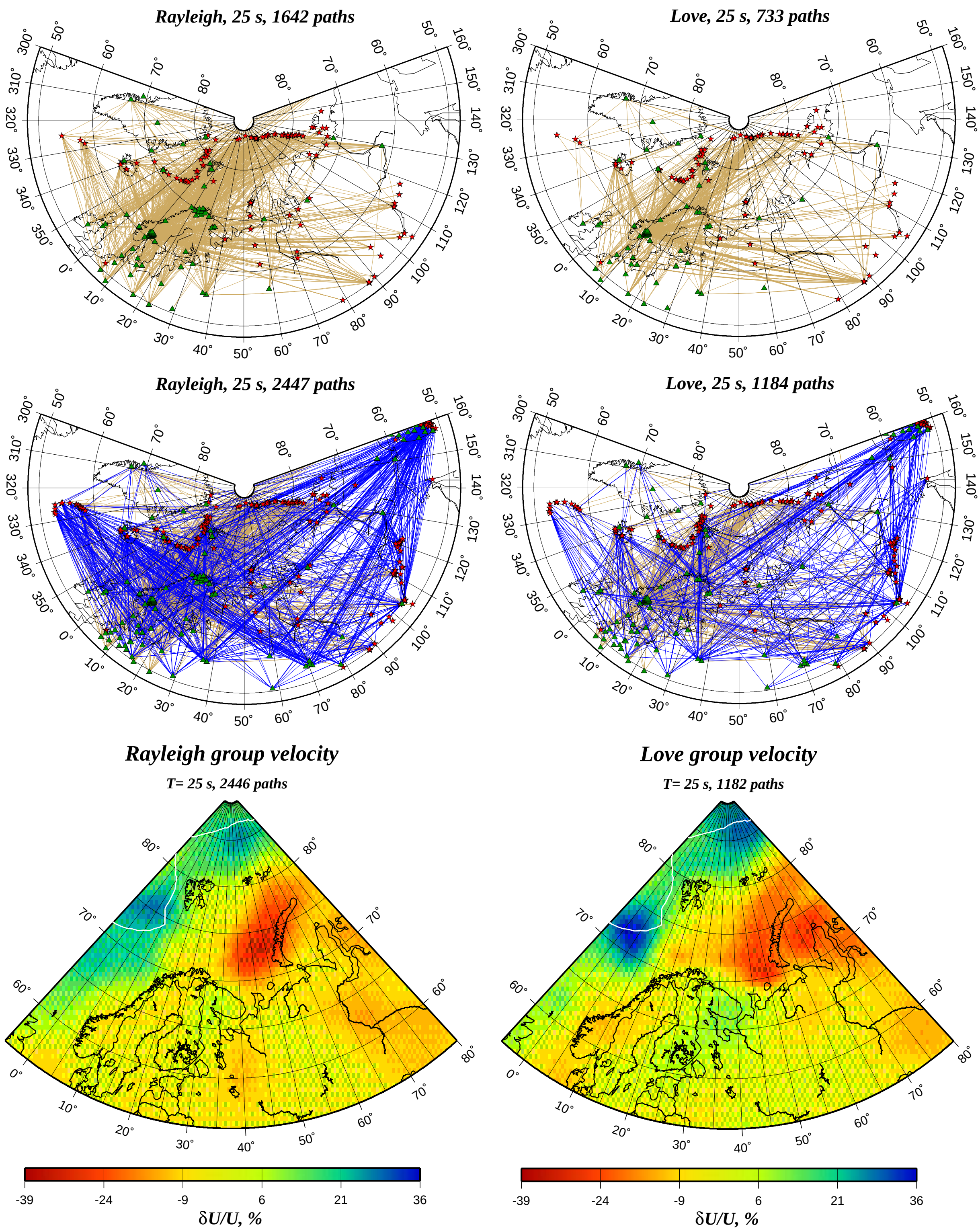

Fig. 6.3.4. Results of the 2D inversion for the group velocities of Love (on the right) and Rayleigh waves (on the left) with a period of 25 s. The two maps at the top show the ray coverage of the newly analyzed data. The two maps in the middle show the same rays plus the rays for the data from the preselected CU data set (blue). The two maps at the bottom present the 2D distribution of the inverted group velocities as deviations from the average velocity (in percent).

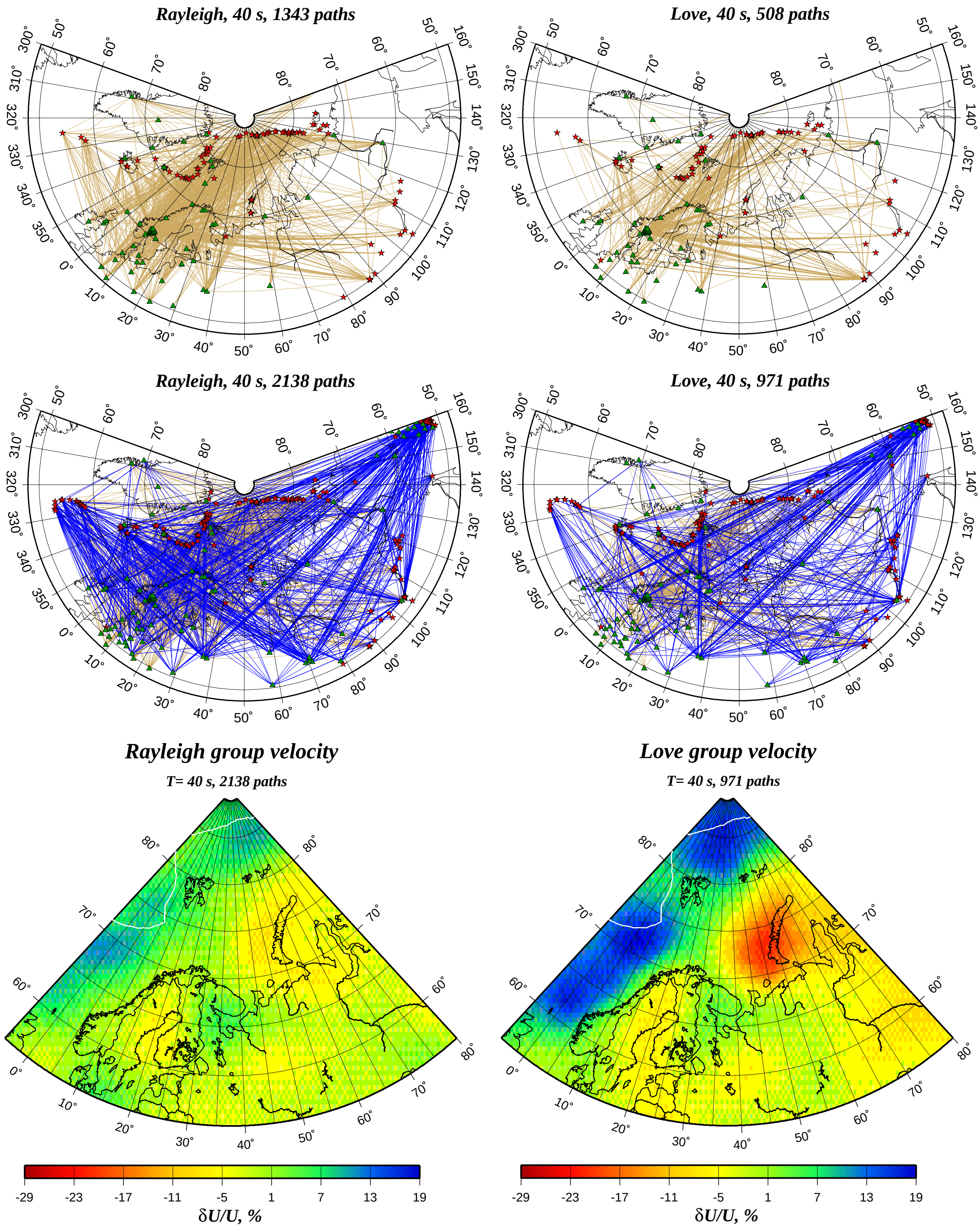

Fig. 6.3.5. Results of the 2D inversion for the group velocities of Love (on the right) and Rayleigh waves (on the left) with a period of 40 s. The two maps at the top show the ray coverage of the newly analyzed data. The two maps in the middle show the same rays plus the rays for the data from the preselected CU data set (blue). The two maps at the bottom present the 2D distribution of the inverted group velocities as deviations from the average velocity (in percent).